

Enhanced Sputtering from the F/Si(100) Surface with Extraction of the Surface Bond Direction

N. Okabayashi,^{1,*} K. Komaki,¹ and Y. Yamazaki^{1,2}¹Graduate School of Arts and Sciences, University of Tokyo, Komaba, Meguro, Tokyo 153-8902, Japan²Atomic Physics Laboratory, RIKEN, Wako, Saitama 351-0198, Japan

(Received 27 March 2011; revised manuscript received 16 June 2011; published 7 September 2011)

It was found that slow highly charged ions had a high ability to ionize F atoms on a F/Si(100)- 2×1 surface and desorb F^+ ions along the local bond direction. Actually, the F^+ ion yields were proportional to the incident charge cubed, and the F^+ ions were emitted along the Si-F bond directions showing a fourfold symmetry pattern. The trigger process of the F^+ formation is discussed based on a charge transfer process of F $2p$ electrons by extending the classical over barrier model. Further, we found that the kinetic energy of highly charged ion induced F^+ ions is lower than that of electron stimulated F^+ ions caused by the removal of a F $2s$ electron.

DOI: 10.1103/PhysRevLett.107.113201

PACS numbers: 34.35.+a, 79.20.Rf

When a slow highly charged ion (HCI) impacts on a solid surface, intriguing phenomena such as a multielectron transfer, an acceleration by the image charge, and a formation of the hollow atom take place due to its large potential energy or strong electric field [1]. The classical over barrier (COB) model has been successfully applied to describe these phenomena for metals, semiconductors, and insulators [2], where the transfer of surface electrons at the Fermi level is considered. When the surface electrons are removed, the target surface experiences a local charge up, which induces the emission of target atoms if the local charge up has a long relaxation time comparing to the sputtering time, which is referred to as a potential sputtering (PS) [3–9]. PS was frequently discussed by analogy with electron stimulated desorption (ESD), e.g., the sputtering of protons [10] and insulators [3]. In order to judge whether the emission mechanism is really the same for PS and ESD, the direct comparison of thoroughly investigated emission processes for an identical surface is important.

In this Letter, we investigate the F^+ sputtering process from the F/Si(100) surface under slow HCI bombardment, where the incident charge, energy, and angle are systematically varied and ESD is examined as a reference. We report that the F^+ yield is proportional to q^γ ($\gamma \approx 3$), and F^+ ions are sputtered along the direction of the Si-F bond. The latter finding is consistent with our electron stimulated desorption ion angular distribution (ESDIAD); however, the kinetic energy of HCI induced F^+ is smaller than that by ESD. We demonstrate that the multiple removal of F $2p$ electrons is important in PS by extending the COB model, which is in contrast to ESD induced by the removal of a F $2s$ electron and is the reason of the different kinetic energy of F^+ ions.

The experimental setup and data acquisition system were described in detail elsewhere [11] and are only briefly repeated here. HCIs were extracted from a compact electron beam ion source (mini-EBIS) [12], charge-state selected with a Wien filter, periodically swept with a

deflector to form a 50 kHz train of 50 ns wide pulses, and guided into a target chamber. A pulsed electron source with the width of 15 ns was prepared to characterize the target surface by ESDIAD technique, which is known to provide information on the bond direction [13]. Positively charged secondary ions released from the target surface were accelerated normal to the surface and were detected by a two-dimensional position- and time-sensitive detector; i.e., the full three-dimensional information on the initial momenta is obtained with the present measurement system [14]. The dose of the HCI to get a set of data was typically 10^8 . Considering that the beam spot size was ≈ 2 mm, the dose density was $\sim 10^9/\text{cm}^2$, which was several orders of magnitude lower than the atomic density of the Si(100) surface, $7 \times 10^{14}/\text{cm}^2$, and the surface deterioration should be negligibly small for all the measurements presented here.

The target was a B-doped Si(100) wafer of $24 \times 14 \times 0.5$ mm³ having resistivity of 18 Ωcm (orientation accuracy $\pm 0.5^\circ$) and was chemically treated to form a thin oxide layer protecting the Si surface from contamination during installation in the target chamber [15]. After the target chamber reached $\approx 2 \times 10^{-10}$ Torr, the oxide layer was removed by heating the sample at ≈ 1170 K 3 times, for 3 min each, which yielded the Si(100)- 2×1 reconstructed surface [16]. Finally, the Si(100)- 2×1 surface at room temperature was exposed to CF_n ($n = 1, 2, 3$) and C_2F_m ($m = 3, 4$) molecules emitted from a heated polytetrafluoroethylene, which yielded a fluorine covered Si surface. ESDIAD of F^+ ions with typical impact energy of 350 eV was applied both before and after the HCI measurements to assure that the F/Si surface was free of deterioration.

It is known that ESDIAD of F^+ ions from a F/Si(100) surface has four peaks in the (011) and (01 $\bar{1}$) planes with fourfold symmetry [17], which is because the Si(100) surface has two domains, one with its Si dimer bond along the [011] and the other along the [01 $\bar{1}$] directions [16]; see

Fig. 1(a). The first-principle calculation predicts that (1) the polar angle of the Si-F bond from the surface normal is 23° and (2) $0.4e^-$ is transferred to the fluorine atom [18]. Prediction (2) indicates that F^+ ions can be emitted when two electrons are removed. Actually, the threshold energy of F^+ emission by ESD process was ≈ 28 eV [17,19], which is close to the transition energy of the F $2s$ state to the conduction band minimum, indicating that F^+ ions are formed via a Coster-Kronig transition such as $F^*(2s^1 2p^6) \rightarrow F^+(2s^2 2p^4) + e^-$ after the removal of the $2s$ electron of a F atom [17,19].

A three-dimensional distribution $f(\varepsilon, \theta, \phi)$ of emitted ions was evaluated combining the time of flight and two-dimensional position information, where ε is the emission energy and θ and ϕ the polar and azimuthal angles, respectively [20]. The emission angle distribution $f(\theta, \phi)$ is obtained by integrating $f(\varepsilon, \theta, \phi)$ over the emission energy ε . Figure 1(b) shows $f(\theta, \phi)$ of F^+ ions for 3.9 keV Ar^{q+} ions ($4 \leq q \leq 7$) where the incident angle, α , with respect to the surface normal is 35° . Like in the case of ESDIAD, four peaks are clearly seen in the (011) and (01 $\bar{1}$) planes. The most probable polar angles of emission extracted from Fig. 1(b) were $22^\circ \pm 4^\circ$ from the surface normal for all the charge states measured ($4 \leq q \leq 7$), which agreed quite well with our ESDIAD value of $23^\circ \pm 2^\circ$. These uncertainties originated primarily from the time zero of the flight time [20]. The polar angle so obtained is consistent with the predicted value of 23° by the first-principle calculation [18]. The full widths at half maximum of each peak in the fourfold structure were 23° , 24° , 26° , and 29° , for $q = 4, 5, 6$, and 7 , respectively, where the effects due to the beam sizes and the pulse widths were corrected for [14].

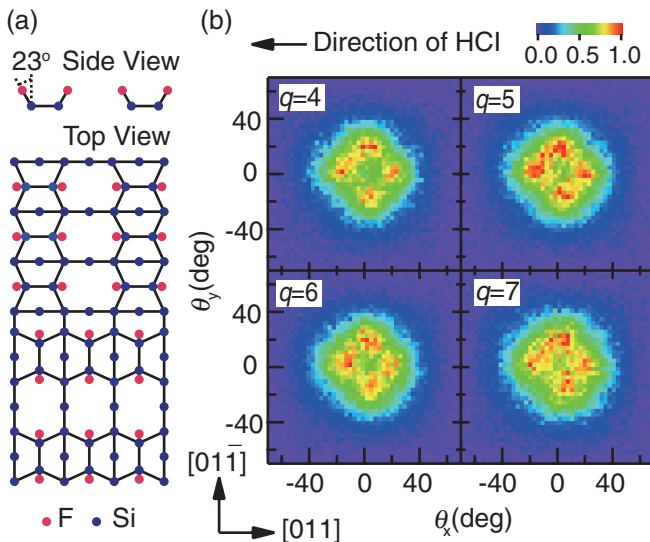


FIG. 1 (color). (a) Schematic diagram of the fluorine adsorbed Si(100) surface. (b) Two-dimensional angular distributions of F^+ ions emitted from the F/Si(100) surface irradiated by 3.9 keV Ar^{q+} ($4 \leq q \leq 7$) ions incident at $\alpha = 35^\circ$. The peak intensity for each distribution is normalized to unity.

Figure 2(a) shows $f(\varepsilon)$ the kinetic energy distribution of F^+ ions for 3.9 keV Ar^{q+} ($4 \leq q \leq 7$) ions with $\alpha = 35^\circ$, which is obtained by integrating $f(\varepsilon, \theta, \phi)$ over the emission angle θ and ϕ . The peak energies for $q = 4, 5, 6$, and 7 were $1.8 \text{ eV} \pm 0.6 \text{ eV}$, $2.0 \text{ eV} \pm 0.6 \text{ eV}$, $2.2 \text{ eV} \pm 0.6 \text{ eV}$, and $2.2 \text{ eV} \pm 0.6 \text{ eV}$, respectively; i.e., the peak energies were independent of q within the error bars originating from the time zero of the time of flight [20]. It was further found that $f(\varepsilon)$ and $f(\theta, \phi)$ of F^+ ions depended neither on the incident energy E ($2.5 \leq E \leq 5.0$ keV) nor on the incident angle α ($22 \leq \alpha \leq 65^\circ$) [14].

Figure 3 shows the yields of F^+ and Si^+ ions as a function of the charge state q of the Ar^{q+} ions ($4 \leq q \leq 8$) incident at $E = 3.2$ keV and $\alpha = 30^\circ$. It is seen that the F^+ yield increases with q like q^γ ($\gamma \approx 3$), although the Si^+ yield is independent of q . Further, the Si^+ yields depended on the incident angle α like $1/(\cos\alpha)^{1.7}$, but the F^+ yields did not depend on α [14]. These behaviors of Si^+ ions are typical for kinetic sputtering phenomena, but those of F^+ ions were quite different. Summarizing these experimental findings: (1) the F^+ emission seems to be triggered by some electron removal processes induced by the charge or the field of the incident ions but not by any kinematical effects, and (2) the emission proceeds following the Si-F bond direction almost independent of the incident charge, energy, and angle.

Here, we consider the trigger process of F^+ emission following the COB model [2] for a F/Si surface [see Fig. 4(a)], where the case of normal incidence is investigated for simplicity. At the critical distance of an HCI from a surface, $R_{Si}(q)$, the electrons in the top of the Si valence band with the work function of 5 eV are resonantly and classically transferred to highly excited states of the HCI. The critical distance is approximately given by

$$R_{Si}(q) \approx 6.7\sqrt{q} + 0.4 \text{ (a.u.)}. \quad (1)$$

The principal quantum number into which the electron is transferred is approximately given by $n_{Si}(q) \approx q + 1$.

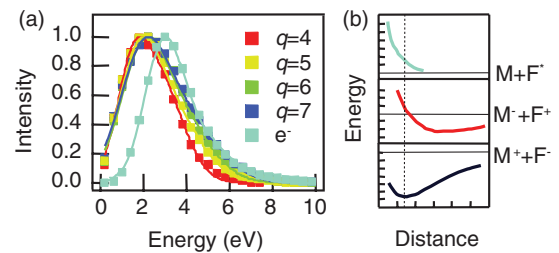


FIG. 2 (color). (a) Kinetic energy distributions of F^+ ions emitted from the F/Si(100) surface irradiated by 3.9 keV Ar^{q+} ($4 \leq q \leq 7$) ions incident at $\alpha = 35^\circ$ and 350 eV e^- . The emission energy of F^+ ions in ESD is stable for the electron energy of 70–750 eV and 50% higher than those in HCI impact. (b) Schematic drawing of potential energy curves for the case of F^+ (red line) and F^* (light blue line), where the former shows the smaller kinetic energy comparing to the latter [22].

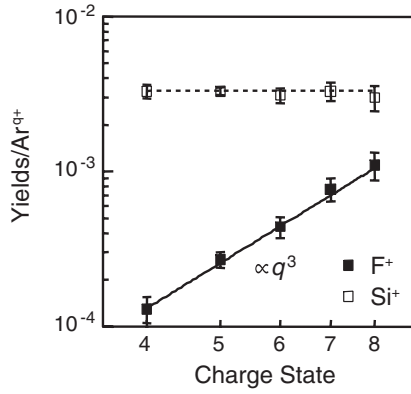


FIG. 3. Incident charge-state dependence of F^+ and Si^+ yields emitted from the F/Si(100) surface irradiated by 3.2 keV Ar^{q+} ions incident at $\alpha = 30^\circ$.

Once an electron is captured, the charge state of the HCI is reduced by the screening of the transferred electron. Thus, the potential barrier between the HCI and the surface gets higher, and the next electron can be transferred after the HCI gets closer to the surface. By this way, electrons are transferred into high Rydberg states one by one, keeping inner shell holes, resulting in a so-called hollow ion (HI) or hollow atom (HA). Assuming a perfect screening of the projectile by transferred electrons [21] and using Eq. (1) to estimate the critical distance for the following electrons, the charge state $q_{Si}(R)$ of the HI or HA at R viewed from the Si valence electrons varies in a stepwise manner, as shown by the green line in Fig. 4(b).

Next, we consider the outermost electrons ($2p$) in the F atom located at $\rho (= 1.6$ a.u.) above the image plane [18], which is assumed to locate 1.3 a.u. (half an atomic layer) above the topmost Si layer [see Fig. 4(a)]. Like in the case for the Si valence electrons, a potential barrier between the fluorine and HCI is formed for the fluorine $2p$ electron. We should note that an effective charge of HI or HA viewed from the fluorine, $q_F(R)$, is different from $q_{Si}(R)$ because the F atom protrudes from the image plane [see Fig. 4(a)]. The effective charge state $q_F(R)$ is approximately given by

$$q_F(R) = q - \sum_n \frac{N_n(R)}{n^2} \sum_{l=0}^{n-1} (2l+1) \times \int_0^{\sqrt{(R-\rho)^2+d^2}} \psi_{nl}^2(r) r^2 dr, \quad (2)$$

where d is the impact parameter, $\psi_{nl}(r)$ is the radial wave function, n is the principal quantum number, l is the orbital angular momentum, and $N_n(R)$ is the number of electrons which have been transferred from the Si valence band to the n shell of the HCI located at R . For the sake of simplicity, the hydrogenlike wave functions were employed for $\psi_{nl}(r)$ in calculating Eq. (2). Deexcitation processes of the HI or HA were neglected because the interaction time is quite short (< 10 fs), as compared

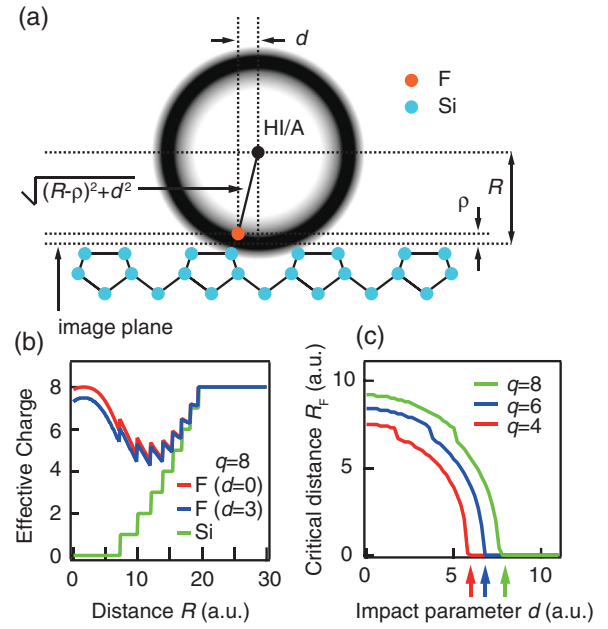


FIG. 4 (color). (a) Schematic drawing of the COB process for the F/Si surface. The HI or HA is located at distance R from the image plane and with the impact parameter of d . The gray area with radius R represents the high density area of the already transferred Si valence electron shared by the HI or HA and the Si substrate. (b) The green line is the charge-state evolutions of HI or HA with the initial charge state $q = 8$ viewed from the silicon (q_{Si}). The red and blue lines are the charge-state evolutions of the same HI or HA viewed from the fluorine atom (q_F), where the impact parameters (d) are 0 and 3 a.u., respectively. (c) Critical distances for the F $2p$ electron transfer are plotted as a function of the impact parameter. The arrows show the upper limit of the impact parameter for the extended COB.

with typical deexcitation time [2]. The red and blue lines in Fig. 4(b) show $q_F(R)$ for two different impact parameters, where $q_F(R)$ decreases slowly, as compared with $q_{Si}(R)$ [green line in Fig. 4(b)], because the orbital radius of HI or HA is larger than the distance between the HCI and the F atom, $\sqrt{(R-\rho)^2+d^2}$ [see Fig. 4(a)]. The critical distance, R_F , is defined as the position of the HCI where the potential barrier height for the fluorine electron gets equal to the binding energy of the F $2p$ electron, $E_{F2p} + \Delta E_F(R)$, where E_{F2p} is the intrinsic binding energy and $\Delta E_F(R)$ is the sum of the positive and negative shifts by the charge of HCI (q_F) and by the image charge of HCI (q_{Si}), respectively. Here, $E_{F2p} = 14$ eV is adopted from the photoelectron spectroscopy [19]. The solid lines in Fig. 4(c) show R_F for different q as a function of the impact parameter, indicating that the classically allowed electron transfer process of the F $2p$ electron can take place competing with that of the Si valence electron, which is referred to as an extended COB model here. As shown by arrows in Fig. 4(c), there are upper limits of impact parameter for the electron transfer of the F $2p$ electron.

As soon as the second electron is transferred from the F $2p$ state, a F^+ ion is formed and is emitted due to the repulsive force in the Si-F bond, which is referred to as the pairwise PS model [10]. In contrast to the pairwise PS model, F^+ emissions observed in ESD were induced by a removal of the F $2s$ electron, i.e., formation of the $F^*(2s^1 2p^6)$ state [17,19]. This F^* can be desorbed by the repulsive interaction with the surface [22] and can be changed into the F^+ state by the Coster-Kronig process on the way of the emission [22]. Avouris *et al.* predicted that the larger kinetic energy of F^+ ions formed via the long-lived F^* state comparing to that of the instantaneously formed F^+ because of the absence of the repulsive image charge [22]; see Fig. 2(b). If we assume that the electron stimulated F^+ is emitted via the long-lived F^* state and the HCI induced F^+ is immediately formed by the collision process, their calculation is consistent with our observation [see Fig. 2(a)]. The time interval between the capture of the first electron from the fluorine and the penetration of HI or HA into the substrate is estimated to be a few fs, which is shorter than the time necessary for the F^+ emission (order of 100 fs). This time difference explains at least qualitatively why the trigger process and the emission process take place independently.

The recoil process of fluorine by the projectile determines the lower limit of the impact parameter, where the F $2p$ electron can be transferred to HI or HA without losing the bond information. For example, the recoil energy of a F atom by an Ar atom with the impact parameter of 2 a.u. is less than the dissociation energy of the Si-F bond (5 eV [18]), where we assume the Thomas Fermi Moliere potential [23] between the F and Ar and neglect the Si atoms around for simplicity. On the other hand, the upper limit of the impact parameter is determined by the extended COB model, which is shown by the arrows in Fig. 4(c). The range of the impact parameter between the upper limit and lower limit can contribute to the PS of F^+ which keeps the bond information.

The probability that the F^+ ions are produced by secondary electrons induced by HCI bombardments is negligibly small because (1) the F^+ emission energy for Ar^{q+} impacts are considerably smaller than those for e^- impacts, i.e., both emission processes are intrinsically different, and (2) the F^+ yield for Ar^{6+} ions was observed to be 2 orders of magnitude larger than the maximum yield for e^- impacts (200 eV) [14], although the secondary electron yields are at most ten [24] and their kinetic energies are mostly smaller than the threshold energy to induce ESD [17,19].

In conclusion, we have investigated the HCI induced F^+ sputtering process by measuring the kinetic energy and the emission angle of the desorbed ions for various charge states. We found that the ionization process of fluorine

and the desorption process of F^+ take place almost independently, and the former shows the strong charge-state dependence and the latter reflects the local bond configuration of the fluorine atom on the Si surface. The extended COB model predicts that the ionization of F $2p$ electrons plays a dominant role in the F^+ sputtering. Further, we found that the kinetic energy of HCI induced F^+ is smaller than that of ESD, which is consistent with the prediction by Avouris *et al.* [22]. Extending the present findings to neutral species dominant in PS [3] is expected to deepen our understanding on sputtering processes.

We are deeply indebted to J. Burgdörfer for his careful reading of the manuscript and valuable comments.

*Present address: Materials and Structures Laboratory, Tokyo Institute of Technology, Yokohama, Kanagawa 226-8503, Japan.

norio@msl.titech.ac.jp

- [1] A. Arnau *et al.*, *Surf. Sci. Rep.* **27**, 113 (1997).
- [2] J. Burgdörfer, P. Lerner, and F. W. Meyer, *Phys. Rev. A* **44**, 5674 (1991).
- [3] F. Aumayr *et al.*, *Int. J. Mass Spectrom.* **192**, 415 (1999).
- [4] S. T. de Zwart *et al.*, *Surf. Sci.* **177**, L939 (1986).
- [5] T. Schenkel *et al.*, *Phys. Rev. Lett.* **80**, 4325 (1998).
- [6] N. Kakutani *et al.*, *Nucl. Instrum. Methods Phys. Res., Sect. B* **96**, 541 (1995).
- [7] K. Kuroki *et al.*, *Appl. Phys. Lett.* **81**, 3561 (2002).
- [8] M. Flores *et al.*, *Phys. Rev. A* **79**, 022902 (2009).
- [9] R. Heller *et al.*, *Phys. Rev. Lett.* **101**, 096102 (2008).
- [10] J. Burgdörfer and Y. Yamazaki, *Phys. Rev. A* **54**, 4140 (1996).
- [11] N. Okabayashi *et al.*, *Nucl. Instrum. Methods Phys. Res., Sect. B* **205**, 725 (2003).
- [12] K. Okuno, *Jpn. J. Appl. Phys.* **28**, 1124 (1989).
- [13] R. D. Ramsier and J. T. Yates, Jr., *Surf. Sci. Rep.* **12**, 246 (1991).
- [14] See Supplemental Material at <http://link.aps.org/supplemental/10.1103/PhysRevLett.107.113201> for figures and tables.
- [15] A. Ishizaka and Y. Shiraki, *J. Electrochem. Soc.* **133**, 666 (1986).
- [16] R. J. Hamers, R. M. Tromp, and J. E. Demuth, *Phys. Rev. B* **34**, 5343 (1986).
- [17] J. Bozack *et al.*, *Surf. Sci.* **184**, L332 (1987).
- [18] C. J. Wu and E. A. Carter, *Phys. Rev. B* **45**, 9065 (1992).
- [19] Ph. Avouris *et al.*, *Mater. Res. Soc. Symp. Proc.* **75**, 591 (1987).
- [20] N. Okabayashi *et al.*, *Nucl. Instrum. Methods Phys. Res., Sect. B* **235**, 438 (2005).
- [21] C. Lemell *et al.*, *Phys. Rev. A* **53**, 880 (1996).
- [22] Ph. Avouris *et al.*, *J. Chem. Phys.* **89**, 2388 (1988).
- [23] G. Moliere, *Z. Naturforsch. Teil A* **2**, 133 (1947).
- [24] H. Kurz *et al.*, *Phys. Rev. A* **48**, 2182 (1993).